Available online at www.sciencedirect.com
SCIENCE DIRECT
ELSEVIER
Journal of the European Ceramic Society 26 (2006) 423–428
ECERS
www.elsevier.com/locate/jeurceramsoc

TiO_2 nanopowders via radio-frequency thermal plasma oxidation of organic liquid precursors: Synthesis and characterization

Ji-Guang Li [a], Hiroshi Kamiyama [a,b], Xiao-Hui Wang [a], Yusuke Moriyoshi [b], Takamasa Ishigaki [a,*]

[a] *Advanced Materials Laboratory, National Institute for Materials Science, Namiki 1-1, Tsukuba, Ibaraki 305-0044, Japan*
[b] *Department of Materials Science, Hosei University, Kajino 3-7-2, Koganei 184-8584, Tokyo, Japan*

Available online 2 August 2005

Abstract

TiO_2 nanopowders have been synthesized via Ar/O_2 thermal plasma oxidation of titanium butoxide (TBO) solutions stabilized with diethanolamine (DEA). Experiments were conducted by varying the O_2 input in the plasma sheath (10–90 L/min) and the DEA/TBO molar ratio (*R*), while keeping the plasma generation power at 25 kW and the reactor pressure at 500 Torr. The resultant powders are mixtures of the anatase and rutile polymorphs in the studied range, whose anatase content and crystallite size exhibit weak dependence on the O_2 input at a fixed *R*. Increasing *R* decreases the anatase content, signifying the role of CO gas, generated via oxidation of the organic precursor, on the phase structure. FE-SEM and TEM analysis show that the resultant powders contain majority of nanoparticles (<50 nm) and some large spheres (>100 nm), whose size and/or number tends to decrease at a higher O_2 input, leading to gradually increased specific surface area. Raman spectroscopy reveals no significant differences in the crystallite size and oxygen-vacancy concentration of the nanocrystals by varying the O_2 input.

Keywords: Powders-gas phase reaction; Precursors-organic; Electron microscopy; TiO_2

1. Introduction

Titania (TiO_2) has been drawing much attention during recent years, due to its unique combination of many interesting photophysical and photochemical properties. The semiconducting oxide is known for its applications in photovoltaic cells and appears to be interesting as a dielectric material for the next generation of ultrathin capacitors due to its high dielectric constant.[1] The relatively high refractive index (2.4–2.9, depending upon the crystalline phase) and good transparency in the visible wavelength region also make the material attractive for photonic band gap (PBG) and other photonic applications.[2,3] Particularly, TiO_2 outstands out from many other semiconducting materials (such as ZnO, CdS, ZnS, and Fe_2O_3) in terms of photocatalytic efficiency, which in combination with its non-toxicity, availability, and chemical stability, makes it very promising as an effective photocatalyst for the de-pollution of air and water as well as the degradation of environmentally harmful organic compounds.[4–6]

The performance of TiO_2 for certain technical application is dominantly influenced by its crystallite size, surface area, phase structure, and impurity (dopant) type and concentration. The industrial production of TiO_2 is mainly by the flame pyrolysis of titanium tetrachloride, which gives diphasic nanopowders containing finer anatase and a small portion of larger rutile crystallites, regardless of the synthesis conditions.[7,8] Various wet-chemical synthetic techniques have been employed to finely tune properties of the resultant TiO_2 powders, including precipitation, sol–gel of inorganic or organic titanium compounds, and hydrothermal treatment.[9] One commonly encountered problem is that these methods may generate amorphous or low crystallinity products, which necessitates a subsequent annealing for crystallization or further crystallization. Such a thermal annealing, however, may

* Corresponding author. Tel.: +81 29 860 4306; fax: +81 29 860 4701.
E-mail address: ISHIGAKI.Takamasa@nims.go.jp (T. Ishigaki).

0955-2219/$ – see front matter © 2005 Elsevier Ltd. All rights reserved.
doi:10.1016/j.jeurceramsoc.2005.07.034

cause hard aggregation and even inter-particle sintering. On the other hand, radio frequency (RF) thermal plasma proves to be a useful tool in the synthesis and surface modification of a wide range of inorganic materials. Its high processing temperature (up to ~15,000 K), superfast quenching rate (~10^5 to ~10^6 K/s), and its high concentrations of chemically reactive radicals provide a unique reaction field for materials processing. Other distinct advantages of plasma processing, in terms of powder synthesis, reside in that the resultant particles are of high purity and are largely dispersed. We report in this work the synthesis of TiO_2 nanoparticles via Ar/O_2 RF thermal plasma oxidation of titanium butoxide (TBO) solutions stabilized with diethanolamine (DEA). The effects of processing parameters (O_2 input and DEA/TBO molar ratio) on powder properties are investigated.

2. Experimental procedure

2.1. Powder synthesis

The experimental apparatus mainly consists of a water-cooled induction plasma torch (Model PL-50, TEKNA Plasma System Inc., Que., Canada), a 2-MHz radio frequency power supply system (Nihon Koshuha Co. Ltd., Japan), a water-cooled stainless steel reactor, and a porous stainless steel filter connecting the reactor and a vacuum pump.

For powder synthesis, a liquid precursor is delivered by a peristaltic pump into the center of the Ar/O_2 plasma plum through an atomization probe. Feeding rate of the precursor is controlled at ~4 mL/min. The liquid precursor is made by adding certain amounts of diethanolamine ($HN(OC_2H_5)_2$) to 0.125 mol of titanium butoxide ($Ti(OC_4H_9)_4$) under water cooling and magnetic stirring. Upon mixing, a weak exothermic reaction is observed, which is attributable to the chelating reaction between the two reagents. Volume of the liquid precursor is then adjusted to 100 mL by adding distilled water. Most of the experiments are made at a DEA/TBO molar ratio of 4, which is the critical value to prevent the hydrolysis of TBO by the intentionally added water or the moisture in air. The Ar/O_2 thermal plasma is generated by mixing O_2 in the Ar sheath. The total flow rate of the sheath gas is kept at 90 L/min, while those of the central and atomizing gases (both pure Ar) are set at 30 and 5 L/min, respectively. The plate power for plasma generation is 25 kW, and the reactor pressure is controlled at ~66.7 kPa.

2.2. Characterization techniques

Phase identification of the resultant powders is performed via X-ray diffractometry (XRD) in conjunction with Raman spectroscopy. XRD analysis is performed on a Rigaku RINT2200V/PC diffractometer (Rigaku, Tokyo, Japan) operating at 40 kV/40 mA using nickel-filtered Cu Kα radiation and a scanning speed of 1.0° 2θ/min. Raman spectroscopy is made using Ar^+ laser excitation (514.5 nm) with a source power of 50 mW and a resolution of 1 cm^{-1} (Model NR-1800, JASCO, Tokyo). Anatase content of the powder is calculated according to the Spurr and Myers equation:[10]

$$f_A = \frac{1}{1 + (1.26 I_R / I_A)} \quad (1)$$

where f_A is the weight fraction of anatase while I_R and I_A denote the rutile (1 1 0) and anatase (1 0 1) reflection intensities. Crystallite size is assayed from the Scherrer equation via X-ray line broadening analysis performed on the anatase (1 0 1) and rutile (1 1 0) diffraction peaks. Specific surface area of the powder is analyzed via Brunauer–Emmett–Teller (BET) analysis (Model Belsorp 18, Bell Japan Inc., Tokyo) via nitrogen chemisorption at 77 K. The specific surface area and equivalent particle size can be correlated by the following equation assuming that the particles are closed spheres with smooth surfaces:

$$S = \frac{6 \times 10^3}{d_{th} D} \quad (2)$$

where d_{th} is the theoretical density of TiO_2 (3.90 g/cm^3 for anatase and 4.27 g/cm^3 for rutile), D (nm) is the average particle size, and S is the specific surface area expressed in m^2/g. Particle morphology is observed via field emission scanning electron microscopy (FE-SEM, Model S-5000, Hitachi, Tokyo) and transmission electron microscopy (TEM, Model JEOL JEM-2000EX, Tokyo).

3. Results and discussion

The TiO_2 nanoparticles formed via instantaneous oxidation of the atomized liquid droplets by Ar/O_2 thermal plasma mainly deposit on the filter and the inner walls of the reactor. Complete oxidation of the organic precursor is achieved at O_2 flow rates ≥10 L/min. The resultant powders exclusively contain TiO_2, and are free from titanium sub-oxide impurities, such as Ti_2O_3, Ti_3O_5, Ti_4O_7 and so on. The powders, however, are mixtures of the anatase and rutile polymorphs, even with pure O_2 (90 L/min) as the plasma sheath. XRD patterns of the powders are shown in Fig. 1 for some typical synthetic conditions. Phase content and crystallite size of the powders are summarized in Table 1 as a function of the O_2 input. It can be seen that the resultant TiO_2 powders show weak dependence on the O_2 flow rate, in terms of phase constituent and crystallite size: the anatase content falls in a narrow range of ~71–78 wt.%, the crystallite size of anatase varies between ~33 and 40 nm, while that of rutile between ~37 and 43 nm. It is known that the metastable anatase phase transforms to thermodynamically stable rutile in the temperature range ~400–1000 °C depending upon a variety of factors mainly including crystallite size, impurity type and concentration, and atmosphere. The formation of anatase as the major phase in this work, despite the high

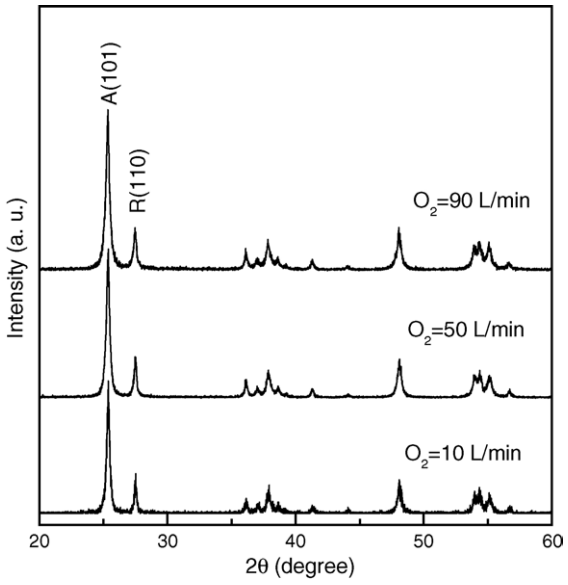

Fig. 1. Typical XRD patterns of the TiO_2 powders formed via Ar/O_2 thermal plasma oxidation of the liquid precursor, with the O_2 flow rate in the sheath indicated. A and R denote the anatase and rutile phases, respectively.

processing temperature, is owing to the superfast quenching effect of the thermal plasma. Theoretical calculations indicate that the metastable anatase phase preferentially nucleates from deeply undercooled TiO_2 melts.[11] Rutile tends to have bigger crystallites than anatase under a given synthetic condition, but the discrepancies are small, typically less than ~5 nm. Rutile is difficult to obtain as nanocrystallites via wet-chemical synthesis of metastable anatase followed by transformation to rutile through the conventional annealing method, as the phase transformation, like the case of Al_2O_3, is characterized by its low nucleation density and extremely fast nuclei growth.[12] The formation of rutile nanocrystallites here is also attributable to the unique superfast quenching effect of the thermal plasma.

Besides serving as an oxidant, O_2 may affect phase structure of the resultant TiO_2 powders in two different ways. One is that the addition of diatomic oxygen gas improves thermal conductivity, leading to enhanced heat transfer from the thermal plasma to the generated TiO_2 particles, which might result in the additional formation of rutile through phase transition. The other is that O_2 directly participates in the phase selection of TiO_2 upon gas phase condensation. Previous work[13,14] on the preparation of TiO_2 via in-flight oxidation of TiN or TiC particles with RF thermal plasma reveals that the rutile phase tends to condense from oxygen-lean titanium oxide gas-clusters while anatase from oxygen-rich clusters. In both the cases, the O_2 flow rate in the plasma sheath affects significantly phase structures of the resultant powders. Through manipulating plasma chemistry, it was shown that both anatase and rutile particles could be obtained in phase-pure form. The different results obtained here apparently derive from the different starting materials used for TiO_2 synthesis. Unlike the cases of TiN and TiC, oxidation of the current organic precursor generates various types of gas species, which may be assigned as CO (CO is more stable than CO_2 at the high temperature of thermal plasma), H_2O, and NO_x for the sake of simplicity. For a DEA/TBO molar ratio of 4, the formation of 1 mol TiO_2 should be accompanied by the release of 32 mol of CO, 40 mol of H_2O, and 4 mol of NO_x. The presence of a large amount of reducing CO gas may generate oxygen-deficient TiO_2 clusters, leading to rutile formation upon condensation. This explains the persistent formation of anatase/rutile phase mixtures irrespective of the amount of O_2 input (Table 1). The simultaneous release of huge amounts of gases into viscous thermal plasma seems to have a masking effect: it protects the resultant TiO_2 particles from exposure to excess O_2. This might account for the weak dependence of phase constituent and crystallite size on the O_2 input.

The ascription of rutile formation to the presence of CO gas is evidenced by the results of comparative studies shown in Fig. 2, in which the preparation conditions and the anatase contents are indicated. Without DEA addition, the anatase content increases from ~75.3 to 79 wt.% (Fig. 2a and b) under the same O_2 input of 10 L/min, due to the reduced CO emission (16 mol CO for per mol TiO_2). On the other hand, raising the DEA/TBO molar ratio from 4 to 16 significantly lowers

Table 1
Anatase content and crystallite size of the products, as a function of the O_2 flow rate in the plasma sheath

O_2 input (L/min)	Anatase content (wt.%)	Crystallite size (nm)		S_{BET} (m^2/g)	S_{XRD} (m^2/g)	φ
		Anatase	Rutile			
10	75.3	36.3	36.5	31.9	41.2	0.77
20	75.3	34.5	38.2	31.6	39.4	0.80
30	70.5	36.3	40.4	29.7	40.1	0.74
40	77.5	36.3	42.8	35.4	40.2	0.88
50	73.2	38.1	42.8	35.3	38.4	0.92
60	71.8	32.9	38.2	39.2	44.0	0.89
70	76.7	38.1	40.4	45.4	39.0	1.16
80	76.0	38.1	42.8	41.7	38.6	1.08
90	76.0	40.2	38.2	48.1	37.9	1.27

DEA/TBO = 4:1 in the precursor solution.

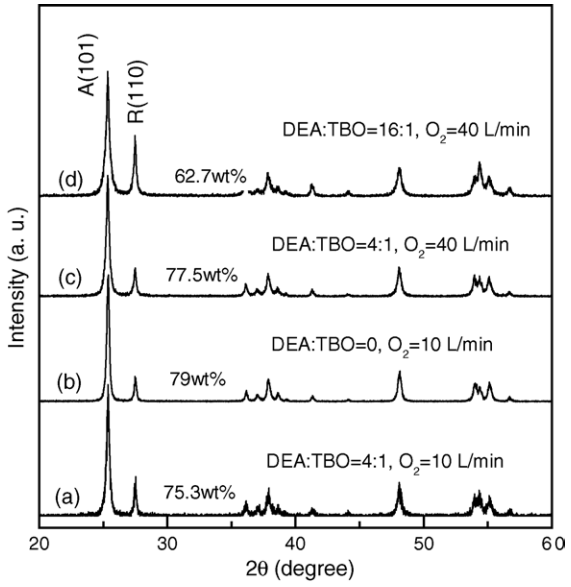

Fig. 2. XRD patterns of the TiO_2 powders, showing the influence of diethanolamine addition on the phase constituent.

the anatase content from ~77.5 to 62.7 wt.% (Fig. 2c and d), as the CO release is greatly increased from 32 to 80 mol for 1 mol TiO_2 formation.

Raman spectroscopy is a useful tool in TiO_2 study, as both the anatase and rutile modifications are sensitive to Raman scattering, which may provide valuable information on the phase composition, crystallinity, crystallite size, and defect (oxygen vacancy) concentrations. Fig. 3 shows Raman spectra of the TiO_2 powders obtained under three typical O_2 flow rates, where positions of the major peaks are indicated

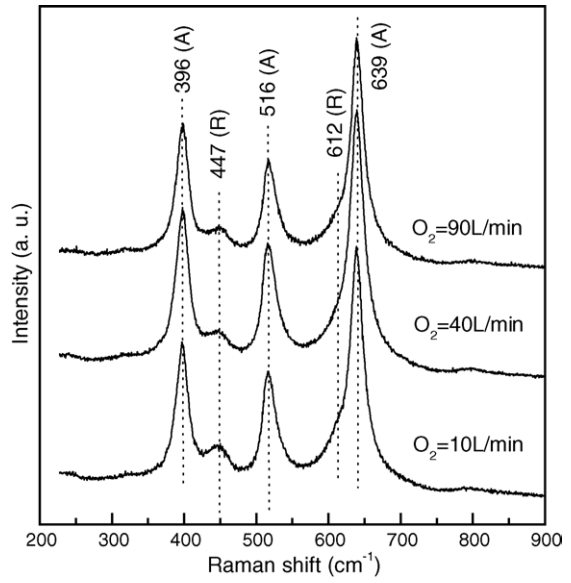

Fig. 3. Raman spectra of the TiO_2 nanopowders synthesized under some typical O_2 input rates. A: anatase; R: rutile.

with dotted lines. The sharp scatterings verify the good crystallinity of the nanoparticles. The strong scatterings peaking at ~396, 516, and 639 cm^{-1} can be well assigned to stoichiometric anatase while that at ~447 cm^{-1} to rutile.[15] The 612 cm^{-1} scattering of rutile overlaps the 639 cm^{-1} scattering of anatase, resulting in the slightly asymmetric broad peak at low wavenumbers. The obtained TiO_2 powders appear slightly gray at lower O_2 inputs (up to 40 L/min) and white at higher O_2 inputs. The slightly gray tint was speculated to be due to the presence of oxygen vacancies. Shifting or broadening of the Raman peaks, however, was not clearly observed, which may imply that the oxygen vacancy concentration is not on a significant level. It was reported that decreasing crystallite size results in wavenumber decrease of the rutile Raman bands and band broadening (decreased peak height to half-width ratio) of both the anatase and rutile modifications.[16] These phenomena were not observed in this work, supporting the weak dependence of crystallite size on processing conditions found via XRD analysis (Table 1).

Particle morphologies are shown in Fig. 4 for the TiO_2 powders synthesized under O_2 flow rates of 40 and 90 L/min. FE-SEM observations (Fig. 4a and b) reveal that the particles are well dispersed and the majority of particles are nanosized (below ~50 nm), though some much larger spheres (>100 nm) are frequently observed. These two distinctly different particle morphologies might arise from the different trajectories of the atomized droplets in the hot zone of the thermal plasma, that is, their different thermal histories. Diameters of the particles, especially the bigger spheres, show clear dependence on the O_2 input in the plasma sheath: a higher O_2 input generates finer powders in overall. Spheres larger than 150 nm are frequently observed in the powder made at O_2 = 40 L/min, but rarely observed in that synthesized at 90 L/min of O_2 input. This might be understood by considering that a higher O_2 input promotes explosive oxidation of the liquid droplets, causing further atomization and hence finer resultant particles. Low-magnification TEM (Fig. 4c) reveals a relatively wide particle size distribution. Most of the particles tend to assume rounded morphologies, and surfaces of the spheres appear smooth. Fig. 4d is the lattice fringe of a hexagonal shaped primary crystallite of ~20 nm observed in the powder shown in Fig. 4c. The spacing of 0.355 nm may correspond to the (1 0 1) plane of anatase (0.352 nm). Besides, amorphous regions up to ~2 nm in thickness are observed along the periphery of the crystallite.

The overall tendency of O_2 input on particle size might be perceived form a factor φ defined as S_{BET}/S_{XRD}, where S_{BET} is the specific surface area assayed via BET and S_{XRD} is the surface area calculated according to Eq. (2) using the average crystallite size determined by XRD. The definition is based upon the facts that BET detects particles while XRD detects crystallites and that φ should approach 1 if each particle is a single crystallite and the particles are monodispersed spheres with smooth surfaces. $\varphi < 1$ indicates crystallite size is smaller

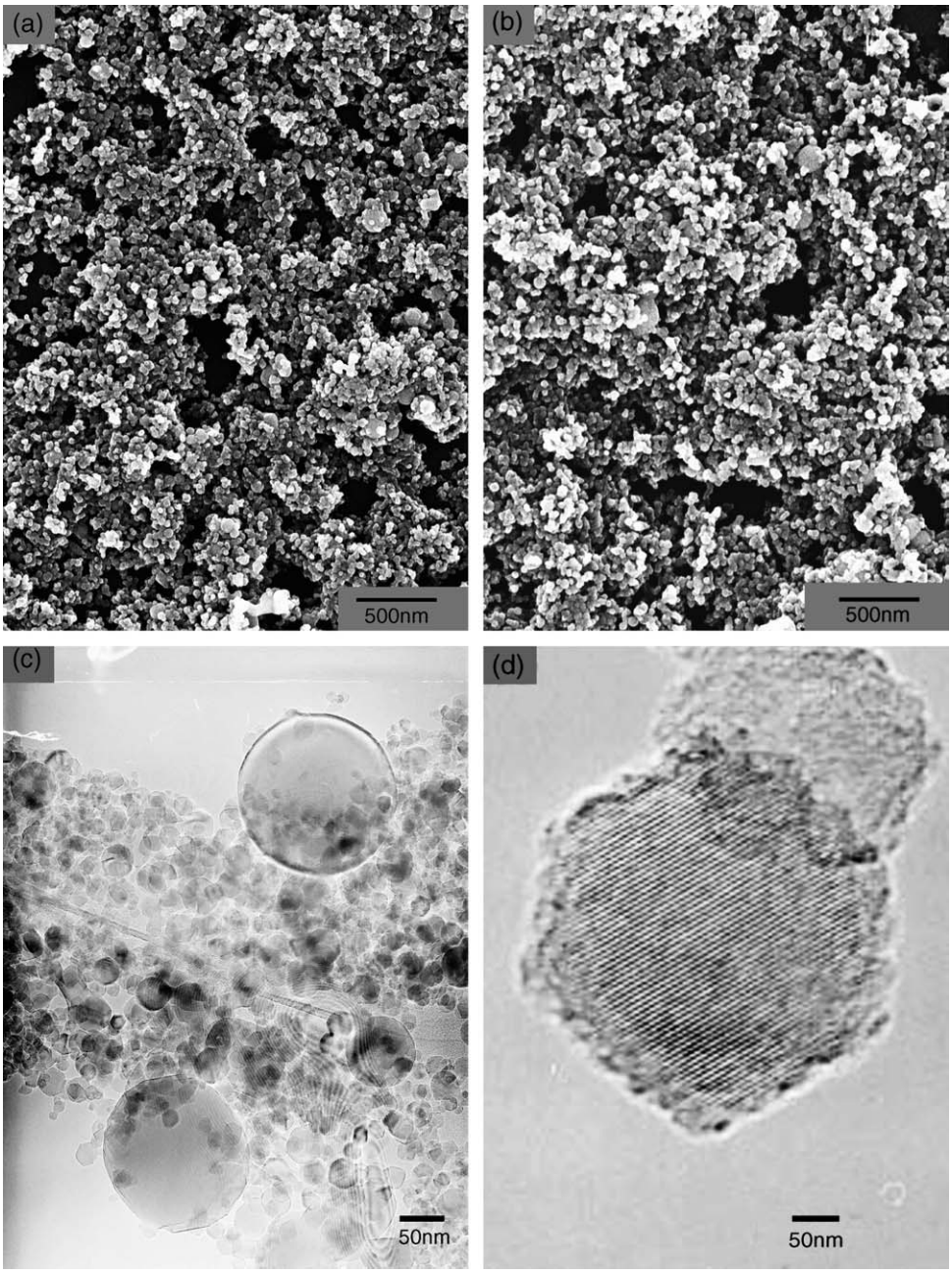

Fig. 4. Electron micrographs showing typical particle morphologies. (a) and (b): FE-SEM images of the powders obtained at O_2 inputs of 40 and 90 L/min, respectively. Notice the different scale-bar lengths; (c) and (d): low- and high-magnification TEM images of the particles shown in (a).

that particle size and hence the presence of hard aggregation, while $\varphi > 1$ holds for monodispersed non-spherical crystallites. The results of calculation are also given in Table 1, from which it can be seen that, though there are some slight fluctuations, the φ value tends to increase at a higher O_2 input. The smaller φ values at lower O_2 inputs are mainly due to the presence of more large dense spheres, which cannot be penetrated by the N_2 gas during BET analysis. The results of φ dependence then imply that the N_2-impenetrable spheres have gradually decreased sizes and/or numbers at higher O_2 inputs, which complies with the results of FE-SEM and TEM observations.

4. Conclusions

Radio frequency Ar/O_2 thermal plasma has been employed to synthesize TiO_2 nanoparticles via combustive oxidation of titanium butoxide solutions stabilized with diethanolamine. Characterizations of the resultant powders were achieved by XRD, BET, Raman spectroscopy, FE-SEM, and TEM analysis. The obtained results are summarized as follows:

(1) The resultant TiO_2 powders are mixtures of the anatase and rutile polymorphs, regardless of the O_2 input in

the plasma sheath (10–90 L/min). The anatase content (∼71–78 wt.%), anatase crystallite size (∼33–40 nm), and rutile size (∼37–43 nm) weakly depend upon the O_2 input. The CO gas released via oxidation of the organic precursor has appreciable effects on the phase constituent.

(2) The majority of the resultant TiO_2 particles are nano-sized (<∼50 nm), though some large spheres (>100 nm) coexist in the powders. A higher O_2 input tends to reduce diameters of the large spheres and maybe also their numbers, leading to increased specific surface area.

(3) As long as complete oxidation of the organic precursor is achieved (>10 L/min of O_2 input), the TiO_2 particles do not differ significantly, in terms of crystallite size and oxygen defect concentration, as revealed via Raman spectroscopy.

References

1. Gonzalez, R. J., Zallen, R. and Berger, H., Infrared reflectivity and lattice fundamentals in anatase TiO_2. *Phys. Rev. B*, 1997, **55**, 7014–7017.
2. Ni, P., Dong, P., Cheng, B., Li, X. and Zhang, D., Synthetic SiO_2 opals. *Adv. Mater.*, 2001, **13**, 437–441.
3. Johnson, S. G. and Joannopoulos, J. D., Designing synthetic media: photonic crystals. *Acta Mater.*, 2003, **51**, 5823–5835.
4. Hagfeld, A. and Gratzel, M., Light-induced redox reactions in nanocrystalline systems. *Chem. Rev.*, 1995, **95**, 49–68.
5. Linsebigler, A. L., Lu, G. and Yates Jr., J. T., Photocatalysis on TiO_2 surfaces: principles, mechanisms, and selected results. *Chem. Rev.*, 1995, **95**, 735–758.
6. Hoffmann, M. R., Martin, S. T., Choi, W. and Bahnemann, D. W., Environmental applications of semiconductor photocatalysis. *Chem. Rev.*, 1995, **95**, 69–96.
7. Akhtar, M. K., Pratsinis, S. E. and Mastrangelo, S. V. R., Dopants in vapor phase synthesis of titania powders. *J. Am. Ceram. Soc.*, 1992, **75**, 3408–3416.
8. Skandan, G., Chen, Y. J., Glumac, N. and Kear, B. H., Synthesis of oxide nanoparticles in low pressure flames. *Nanostruc. Mater.*, 1999, **11**, 149–158.
9. Klein, S. M., Choi, J. H., Pine, D. J. and Lange, F. F., Synthesis of rutile titania powders: agglomeration, dissolution, and reprecipitation phenomena. *J. Mater. Res.*, 2003, **18**, 1457–1464.
10. Spurr, R. A. and Myers, H., Quantitatively analysis of anatase–rutile mixture with an X-ray diffractometer. *Anal. Chem.*, 1957, **29**, 760–765.
11. Li, Y. L. and Ishigaki, T., Thermodynamic analysis of nucleation for anatase and rutile from TiO_2 melt. *J. Crystal Growth*, 2002, **242**, 511–516.
12. Lee, G. H. and Zuo, J. M., Growth and phase transformation of nanometer-sized titanium oxide powders produced by the precipitation method. *J. Am. Ceram. Soc.*, 2004, **87**, 473–479.
13. Li, Y. L. and Ishigaki, T., Controlled one-step synthesis of nanocrystalline anatase and rutile TiO_2 powders by in-flight thermal plasma oxidation. *J. Phys. Chem. B*, 2004, **108**, 15536–15542.
14. Oh, S. M. and Ishigaki, T., Preparation of pure rutile and anatase TiO_2 nanopowders using RF thermal plasma. *Thin Solid Films*, 2004, **457**, 186–191.
15. Zhang, Y. H., Chan, C. K., Porter, J. and Guo, W. J., Micro-Raman spectroscopic characterization of nano-sized TiO_2 powders prepared by vapor hydrolysis. *J. Mater. Res.*, 1998, **13**, 2602–2609.
16. Cheng, H., Ma, J., Zhao, Z. and Qi, L., Hydrothermal preparation of uniform nanosize rutile and anatase particles. *Chem. Mater.*, 1995, **7**, 663–671.